Catalysis Today 174 (2011) 37–45

Contents lists available at ScienceDirect

Catalysis Today

journal homepage: www.elsevier.com/locate/cattod

Recycling of dual hazardous wastes in a catalytic fluidizing process

Yeuh-Hui Lin[a,b,*], Chun-Chieh Tseng[c], Ta-Tung Wei[a,b], Chia-Tse Hsu[a,b]

[a] Institute of Chemical and Biochemical Engineering, Kao Yuan University, Kaohsiung 840, Taiwan
[b] Department of Greenergy Science and Technology, Kao Yuan University, Kaohsiung 840, Taiwan
[c] Department of Chemistry, National Kaohsiung Normal University, Kaohsiung 824, Taiwan

ARTICLE INFO

Article history:
Received 26 October 2010
Received in revised form 8 April 2011
Accepted 19 April 2011
Available online 14 June 2011

Keywords:
Catalyst
Pyrolysis
Hazardous
Fluiding
Selectivity

ABSTRACT

A mixture of post-consumer polyethylene/polypropylene/polystyrene (PE/PP/PS) with polyvinylchloride (PVC) waste was pyrolyzed over cracking catalysts using a fluidizing reaction system in an FCC process operating isothermally at ambient pressure. The influences of catalyst types and reaction conditions including reaction temperatures, ratios of catalyst to plastic feed, flow rates of fluidizing gas and catalyst particle sizes were examined. A model based on kinetic and mechanistic considerations associated with chemical reactions and catalyst deactivation in the acid-catalyzed degradation of plastics has been developed. The results of this study are useful for determining the effects of catalyst types and reaction conditions on both the product distribution and selectivity from commingled plastic waste, and especially for the utilization of post-use commercial FCC recycled catalysts for producing valuable hydrocarbons in a fluidizing cracking process. Moreover, the use of this recycled/modified FCC spent catalyst (RCat-s1) together with an optimal reaction system can be an adequate option since it may lead to a cheaper process with valuable products and can also be further used as a dual recycling of chlorine-containing hazardous waste plastics and a post-use commercial catalyst waste from FCC refinery.

1. Introduction

It is undesirable to dispose of waste plastics by landfill due to high costs and poor biodegradability [1]. An alternative strategy is that of chemical recycling, known as feedstock recycling or tertiary recycling, which has attracted much interest recently with the aim of converting waste plastics into basic petrochemicals to be used as chemical feedstock or fuels for a variety of downstream processes. Two main chemical recycling routes are the thermal and catalytic degradation of waste plastics [2]. The thermal degradation of plastics to low molecular weight materials has a major drawback in that a very broad product range is obtained. In addition, these processes require high temperatures typically more than 500 °C and even up to 900 °C. These facts strongly limit their applicability and especially increase the higher cost of feedstock recycling for waste plastic treatment. Therefore, catalytic degradation provides a means to address these problems. The use of catalyst is expected to reduce reaction temperature, to promote decomposition speed, and to modify the products [3–5]. Catalysts for plastic cracking may be either homogeneous or heterogeneous, although the former are rather more the exception than the rule owing to the problem of recovery and separation of the catalysts from the products. This is not the case for heterogeneous system. The catalytic degradation of polymeric materials has been reported for a range of model catalysts centered on the active components in a range of different catalysts, including zeolite-based such as ZSM-5, BEA, US-Y, MOR, and modified nanocrystalline of Y, and ZSM-5 [6–11], amorphous silica-aluminas (SAHA) and the family of mesoporous MCM materials [12–15]. However, these catalysts have been used that even if performing well, they can be unfeasible from the point of view of practical use due to the cost of manufacturing and the high sensitivity of the process to the cost of the catalyst.

An economical improvement of recycling the plastic waste using catalytic cracking can operate in mixing the plastic waste with fluid catalytic cracking (FCC) commercial catalysts. In typical commercial application for refinery, the ZSM-5 zeolite crystals are mixed with an amorphous matrix material such as silica-alumina, which confers on the finished utilization the physical properties required for an FCC catalyst. Ultrastable Y (USY) with lower Y framework alumina contents and hence lower unit cell sizes, tend to produce more light alkenes, mainly at the expense of gasoline. Spent catalysts form a major source of solid wastes in the petroleum refining industries. Due to environmental concerns, increasing emphasis has been placed on the development of recycling processes for the waste catalyst materials as much as possible. A more attracting is that of adding plastic waste into the FCC process, under suitable process-

* Corresponding author at: Institute of Chemical and Biochemical Engineering, Kao Yuan University, No. 1821, Chung-Shan Rd., Kaohsiung 840, Taiwan.
Tel.: +886 7 6077777; fax: +886 7 6077788.
E-mail address: lin@cc.kyu.edu.tw (Y.-H. Lin).

0920-5861/$ – see front matter © 2011 Elsevier B.V. All rights reserved.
doi:10.1016/j.cattod.2011.04.029

Table 1
Catalysts used in the catalytic degradation of post-consumer waste plastics (WPs#4).

Catalyst	Si/Al	Surface area (m^2/g)			Pore size (nm)	Acidity[b]	
		BET[a]	Micropore	External		T_{max} (°C)	m mol NH_3/g
RCat-s1[c]	2.4	139	101	38	n/a	345	0.13
Silicalite	>1000[d]	362	297	65	0.55 × 0.51	n/a	<0.01
HUSY	5.7	472	375	118	0.74	376	0.83
ZSM-5	17.5	375	257	118	0.55 × 0.51	386	0.52
SAHA	2.6	268	21	247	3.28	305	0.24

[a] Total surface area (BET).
[b] Calculated by ammonia TPD measurements.
[c] RCat-s1 after reactive process described in Section 2.1 materials preparation. The Fe/Al ratio of the obtained sample is 0.25 determined by ICP analysis.
[d] Determined by the experimental limits of elemental analysis for Al and Si.

ing conditions with the use of zero value of spent FCC catalysts, a large number of polymers can be economically converted into valuable hydrocarbons. The configuration of the pyrolysis-reforming reactors poses serious engineering and economics constraints. The use of fixed beds or adiabatic batch where plastic and catalyst are contacted directly leads to problems of blockage and difficulty in obtaining intimate contact over the whole reactor. Additionally, the low thermal conductivity and high viscosity of plastics may lead to the appearance of mass and heat-transfer constraint. These factors influence the product distribution along with the operation conditions. For this purpose, a laboratory fluidized-bed reactor has been used to study catalytic cracking of plastics without polyvinyl chloride (PVC) materials by limiting the contact between primary volatile products and the catalyst/plastic mixture [16]. The results of these studies provide the improvement of reactor performance and catalyst utilization; unfortunately, there is still a need to develop kinetic/mechanistic models to describe the experimental results and to facilitate the further development of a process to industrial scale. Moreover, tertiary recycling of mixed plastic wastes containing PVC release hydrogen chloride which causes not only corrosion of the equipment but also the formation of chloro-organic compounds in hydrocarbons. The processing of highly commingled plastics with different compositions within the waste matrix would meet significant technical challenges. A more difficult task is recycling of commingled post-consumer plastic waste since it consists of hydrocarbons and chloride-containing mixed plastics as well as some modified materials. Technology using thermal/catalytic pyrolysis toward valuable hydrocarbons shows a promising future especially for considering the chlorine from residual PVC in the waste [17]. Therefore, it is the objective of this work to investigate a similar FCC reaction system using an Fe modified FCC spent catalyst (RCat-s1) and a series of reaction conditions for the study of the product distributions in the degradation of plastic waste with hazardous PVC mixture (PE/PP/PVC/PS) and for development of a suitable reaction model and an adequate alternative for achieving post-consumer plastic recycling.

2. Experimental

2.1. Materials and reaction preparation

The mixture of waste plastics (WPs#4) used in this study was obtained from post-consumer healthcare plastic waste stream in North-Taiwan with the component of polyethylene (~62 wt% PE = ~38 wt% HDPE + ~24 wt% LDPE), polypropylene (~34 wt% PP), polyvinyl chloride (~3 wt% PVC) and with about 1 wt% polystyrene (PS) mixtures. Typically, the content of waste plastic sample tested by ultimate analysis was about 84.54% C, 12.71% H, 2.62% Cl, 0.06% O, 0.07% N, and 0.13% S. The spent catalyst was first washed with naphtha and then extracted with toluene in a soxhlet apparatus to remove the residual materials. The recycled/modified FCC spent catalyst (RCat-s1) was then prepared by the conventional ion-exchange method [18]. Before being used for ion exchange, it was washed thoroughly to remove residual sodium from the extra lattice. A quantity of recycled FCC spent catalyst was added to H_2O under the nitrogen atmosphere, and then slowly added $FeSO_4$–$7H_2O$ to the slurry within 6 h. The pH of the slurry was kept at 6.8 ± 7.0. After 48 h, it was vacuum filtered, washed and air dried. All the other catalysts were also crushed and sieved to obtain particle sizes to give particle sizes ranging from 75 to 180 μm. All the catalyst was then dried by heating in flowing nitrogen (50 ml min^{-1}) to 120 °C at 60 °C h^{-1}. After 2 h the temperature was increased to 520 °C at a rate of 120 °C h^{-1} to active the catalyst for 5 h. The catalysts employed are described in Table 1. Surface area, pore volume and pore size distribution were measured from the adsorption–desorption isotherms of nitrogen at 77 K on a Micromeritics ASAP 2020 apparatus. Total surface area of the catalysts was estimated by application of the BET equation and total pore volumes from the nitrogen adsorbed at $p/p^o = 0.99$. Pore size distribution was obtained following the BJH model, whereas the micropore specific surface area and the micropore volume were calculated by the *t*-plot method. The acid properties of these catalysts were determined by ammonia temperature-programmed desorption (TPD) in a Micromeritics AutoChem 2910 (TPD/TPR) instrument. The samples were initially purged by heating from ambient temperature to 570 °C under a He flow (50 N ml min^{-1}) at a rate of 10 °C min^{-1} up to 570 °C and remaining at this temperature for 60 min. After cooling to 180 °C, an ammonia flow of 30 N ml min^{-1} was passed through the sample for 30 min. The physisorbed ammonia was eliminated by flowing He at 180 °C for 100 min, whereas the chemically adsorbed ammonia was determined by recording its desorption upon increasing the temperature up to 550 °C with a heating rate of 10 °C min^{-1}, and holding this temperature constant for 30 min. In these treatments, the ammonia concentration in the effluent He stream was measured continuously with a thermal conductivity detector (TCD). High purity nitrogen was used as the fluidizing gas and the flow was controlled by a needle valve and preheated in the bottom section of the reactor tube. Before catalytic pyrolysis experiments were started, several fluidization runs were performed at ambient temperature and pressure to select: (i) suitable particle sizes (both catalyst and polymer waste) and (ii) optimize the fluidizing gas flow rates to be used in the reaction. The particle size of both catalyst (75–180 μm) and plastic mixture (75–250 μm) were chosen to be large enough to avoid entrainment but not too large as to be inadequately fluidized. High flow rates of fluidizing stream improve catalyst–polymer mixing and external heat transfer between the hot bed and the cold catalyst. On the other hand, an excessive flow rate could cause imperfect fluidization and considerable entrainment of fines.

2.2. Experimental procedures and product analysis

A process flow diagram of the experimental system is given elsewhere [16] and shown schematically in Fig. 1. A three-zone

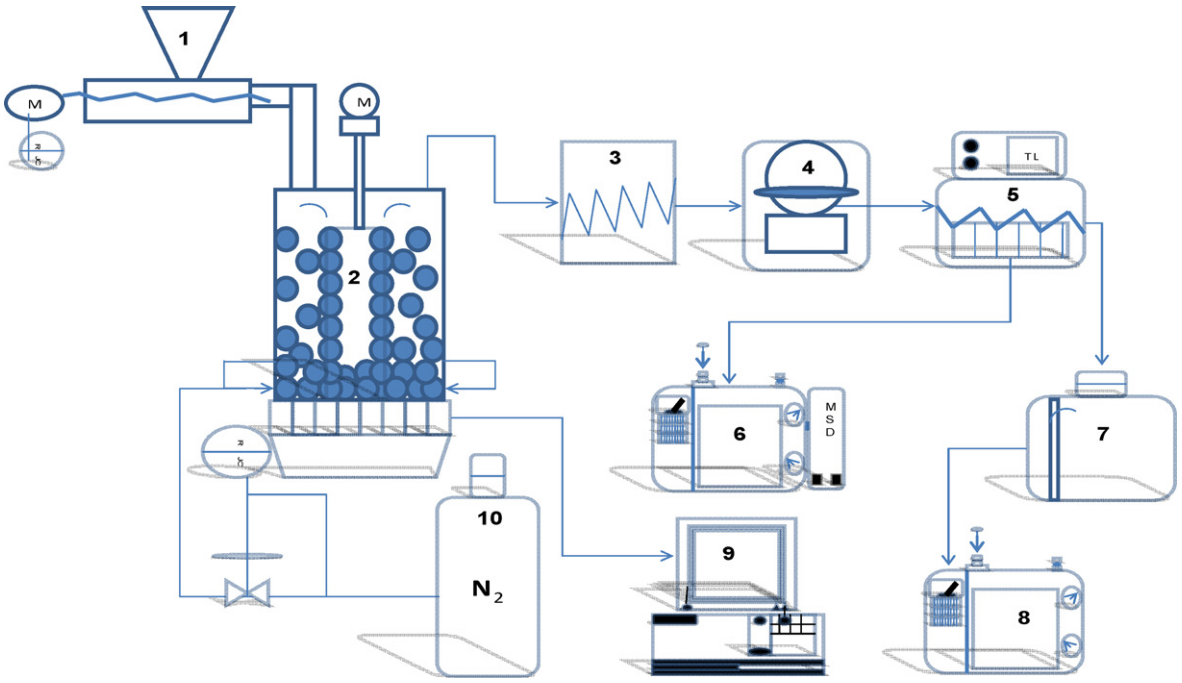

Fig. 1. Schematic diagram of a catalytic fluidizing system for plastic waste recycling: 1. Feeder; 2. Reactor with digital controller for three-zone furnace; 3. Condenser; 4. Online muti-loop automated sample system; 5. Separator; 6. GC/MS analysis of liquid products; 7. Gas bag; 8. GC analysis of volatile products; 9. TG analysis of residue products; 10. N2 fluidizing gas with mass flow control.

heating furnace with digital controllers was used and the temperatures of the furnace in its upper, middle and bottom zones were measured using three thermocouples. By these means the temperature of the pre-heated nitrogen below the distributor and catalyst particles in the reaction volume could be effectively controlled to within ±1 °C. The polymer feed system was designed to avoid plugging the inlet tube with melted polymer and to eliminate air in the feeder. The feed system was connected to a nitrogen supply to evacuate polymer into the fluidized catalyst bed. Thus, commingled polymer particles were purged under nitrogen into the top of the reactor and allowed to drop freely into the fluidized bed at $t = 0$ min. Volatile products leaving the reactor were passed through a glass-fiber filter to capture catalyst fines, followed by an ice-acetone condenser to collect any condensable liquid product. A de-ionized water trap was placed in series after the condenser to catch any HCl produced by the degradation of PVC component. A three-way valve was used after the condenser to route product either into a sample gas bag or to an automated sample valve system with 16 loops. The Tedlar bags, 15 L capacity, were used to collect time-averaged gaseous samples. The bags were replaced at intervals of 10 min, throughout the course of reaction. The multiport sampling valve allowed frequent, rapid sampling of the product stream when required. Spot samples were collected and analyzed at various reaction times ($t = 1$, 2, 3, 5, 8, 12, 15, 20 min). The rate (R_{gp}, wt% min^{-1}) of hydrocarbon production of gaseous products collected by automated sample system in each run was defined by the relationship:

$$R_{gp} = \frac{\text{hydrocarbon production rate of gaseous products in each spot run (g/min)} \times 100}{\text{total hydrocarbon production of gaseous products over the whole spot runs (g)}}$$

Gaseous hydrocarbon products were analyzed using a gas chromatograph equipped with a thermal conductivity detector (TCD) fitted with a 1.5 m × 0.2 mm i.d. Molecular Sieve 13X packed column and a flame ionization detector (FID) fitted with a 50 m × 0.32 mm i.d. PLOT Al_2O_3/KCl capillary column. A calibration cylinder containing 1% C_1–C_5 hydrocarbons was used to help identify and quantify the gaseous products. The solid remaining deposited on the catalyst after the catalytic degradation of the polymer was deemed "residues" and contained involatile products and coke. The amount and nature of the residues was determined by thermogravimetric analysis (TGA). A number of runs were repeated in order to check their reproducibility.

2.3. Kinetic/mechanistic modeling

A general mechanistic reaction scheme involving the discussion of the carbenium ion of catalytic cracking chemistry for the degradation of hydrocarbon has been proposed. This representation is simplified regarding the formation of carbenium ions in that it concentrates on reaction paths rather than on surface species. Theoretical studies suggest that, for the conversion of hydrocarbons on active zeolites, reactions proceed via carbenium ions as transition states (rather than as intermediates) and product distributions are also generally in agreement with carbenium ion studies, although there is still debate about the actual mode of scission. In this paper, a kinetic/mechanistic model including the main mechanistic features and kinetic reaction schemes for plastic degradation over cracking catalysts is investigated (Fig. 2). The model uses the following assumptions.

(i) The liquid-phase plastic. Initially, solid polymer is freely dropped into the reactor and immediately melts to disperse around the catalysts. The molten plastic, in contact with the catalyst particle forms a polymer/catalyst complex, reaction commencing at the surface. Plastic melting and spread times are negligible.

(ii) Evolution of intermediates. Scission reactions generate intermediates which include long-chain olefins and intermediate precursors for carbenium ions. The carbenium ions rapidly

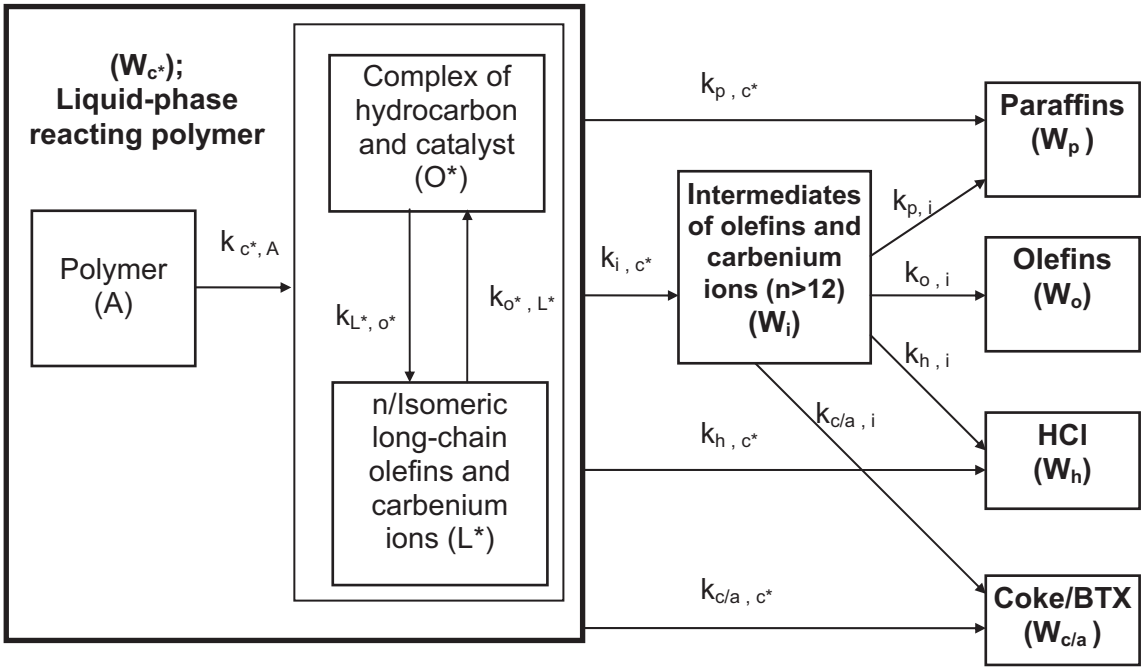

Fig. 2. A kinetic/mechanistic scheme representing the acid-catalyzed degradation of waste plastics (WPs#4) over various cracking catalysts.

reach a steady-state concentration. Alkanes may be generated, via hydrogen transfer, and initially will be largely long-chain products. In general, the number of active sites limits the number of carbenium ion precursors.

(iii) Evolution of products. Once the intermediates are produced, further reactions could be expected to produce smaller chain olefins in equilibrium with surface carbenium ions, as well as alkanes, BTX (Benezene, Toluene and Xylene) and coke. The equilibrium mixture of olefins and carbenium ions subsequently reacts further to produce the final products.

On the basis of the reaction pathway shown in Fig. 2, the rate of formation, $r_{i,j}$, of the product i from reactant r, through reaction j can be written as

$$r_{i,j} = k_{i,j} W_r{}^{n_j} \eta_j \tag{1}$$

where $k_{i,j}$ is the rate constant of the product i from the jth reaction, W_r is the weight fraction of the reactant r present on the acid sites, η_j is the catalyst activity decay of the jth reaction, n_j is the reaction order of the jth reaction. Polymer cracking is known to proceed over acidic catalysts by carbocation mechanisms, where the initially formed ions undergo chain reactions via processes, such as scission or β-scission and isomerization and hydrogen-transfer alkylation and oligomerization, to yield typically smaller cracked products. For plastic waste degradation over a spent fluidizing catalytic cracking (FCC) catalyst, an exponential decay function with activity decaying as function of coke on catalyst was reported previously [19].

$$\eta = \exp[-\alpha C(c)] \tag{2}$$

where $C(c)$ is coke content deposited on the catalyst. For the model we consider, as an approximation, that α, in the deactivation process, can be taken as constant for both polymers and that the active sites are deactivated at the same rate for the acid catalysts studied. The activity decay, η_j, was assumed to be the same for all reaction steps with the activity proportional to the number of remaining sites.

$$\eta_j = \eta = \exp(-\alpha W_r) \tag{3}$$

where W_r is coke content deposited on the individual catalyst. Eqs. (4)–(9) were obtained assuming that reaction rates can be represented by simple first-order processes and catalyst deactivation involving six simultaneous equations. Initially, surface reaction forms a complex of molten plastic/catalyst. Thus, the rate of the consumption of the lumped liquid-phase polymer species (W_{c^*}) can be written as

$$\frac{-dW_{c*}}{dt} = \eta(k_{i,c*} + k_{p,c*} + k_{h,c*} + k_{c/a,c*})W_{c*} \tag{4}$$

Therefore, the formation of intermediates of olefins and carbenium ions can be expressed as

$$\frac{dW_i}{dt} = \eta[(k_{i,c*}W_{c*}) - (k_{o,i} + k_{p,i} + k_{h,i} + k_{c/a,i})(W_i)] \tag{5}$$

Similarly, the evolution of the olefinic lump (W_o), the paraffinic lump (W_p), the HCl lump (W_h), and the coke/BTX lump ($W_{c/a}$) are described as follows

$$\frac{dW_o}{dt} = \eta k_{o,i} W_i \tag{6}$$

$$\frac{dW_p}{dt} = \eta[k_{p,i}(W_i) + (k_{p,c*}W_{c*})] \tag{7}$$

$$\frac{dW_h}{dt} = \eta[k_{h,i}(W_i) + (k_{h,c*}W_{c*})] \tag{8}$$

$$\frac{dW_{r/a}}{dt} = \eta[(k_{c/a,i}(W_i) + (k_{c/a,c*}W_{c*})] \tag{9}$$

The mass balance can be written as

$$\frac{-dW_{c*}}{dt} = \frac{dW_i}{dt} + \frac{dW_o}{dt} + \frac{dW_p}{dt} + \frac{dW_h}{dt} + \frac{dW_{c/a}}{dt} \tag{10}$$

Eqs. (4)–(10) were numerically integrated by a fourth-order Runge–Kutta algorithm with Matlab to very the individual rate constants by minimizing the sum of the squared deviations between calculated and experimental results. This gave values for the apparent rate constants. The kinetics involved is associated with the diffusion of bulky fragments for the unreacted or partially reacted polymer softened by dissolution of low molecular species deposited on the catalyst. Each trend of fluidizing cracking behaviors over

various catalysts may be expressed on a similar reaction pathway following the routes: the formation of a polymer/catalyst complex → the evolution of intermediates → the evolution of products. For the mechanism used in this study, the plastic coating the particles is stated to be liquid, and for the reactions that occur on the interior pore surface the situation would seem to be completed. Gaseous products are forced out to have diffused in the macroporos and produced on the interior surface.

3. Results and discussion

3.1. Degradation of mixture of waste plastics (WPs#4) over various catalysts

Both the carbon number distribution of the products of post-consumer PE/PP/PVC/PS waste plastics (WPs#4) cracking at 390 °C over various catalysts and the nature of the product distribution were found to vary with the catalyst used. As shown in Table 2, the yield of volatile hydrocarbons for zeolitic catalysts (ZSM-5 > HUSY) gave higher yield than non-zeolitic catalysts (SAHA) and zeolite-based modified FCC catalyst (RCat-s1), and the highest was obtained for ZSM-5 (88.3 wt%). Overall, the bulk of the products observed with these acidic cracking catalysts (RCat-s1, HUSY, ZSM-5 and SAHA) were in the gas phase with less than 4 wt% liquid collected. The highest level of unconverted plastic was observed with RCat-s1 and SAHA about 11–12 wt%, while the highest coke yields were observed with HUSY (4.5 wt%). The differences in the product distributions between those catalysts can be seen with ZSM-5 producing a much more C_1–C_4 hydrocarbon gases (nearly 55 wt%) than RCat-s1, HUSY and SAHA catalysts. Some similarities were observed between RCat-s1 and SAHA with C_1–C_4 and C_5–C_9 yields, which were approximately 24–30 wt% and 52–55 wt%, respectively.

A large amount of solid residue, presumably unconverted commingled plastic mixture and high molecular weight degradation products, remained on the spent catalyst was observed at 390 °C for the mixture of commingled plastic degradation over silicalite (Si/Al > 1000, sodium form of siliceous ZSM-5 containing very few or no catalytically active sites). As also can be seen in Table 2, the conversion was only 13.5 wt% for silicalite compared with 82.4 wt% when regenerated and reactive FCC commercial equilibrium catalyst (RCat-s1) was used. Typically thermal degradation productions were observed with silicalite showing primary cracking products (HCl and styrene) and an even spread of carbon numbers (C_1–C_4 = 6.8 wt% and C_5–C_9 = 6.2 wt%) with some isomerization of BTX (0.4 wt%). However, product distributions with RCat-s1 catalyst at 390 °C contained more gasoline materials in the range of C_5–C_9 (54.8 wt%) with 24.3 wt% C_1–C_4 light gases. In this study, the chlorine was chemically separated from the PVC component and as a hydrochloric acid (HCl) in de-ionized water system. The major products of PVC cracking over various catalysts were hydrogen chloride (1.8–2.5 wt%) with light aromatics and smaller chain olefins and paraffins, and with some amount of residue products (involatile residue and coke formation over the reaction) deposited on the catalyst. For acid-catalyzed degradation of polystyrene within plastic mixture, the main products were styrene at about 0.5–08 wt% with some smaller chain volatile hydrocarbons. The rate of gaseous hydrocarbon evolution further highlights the slower rate of degradation over SAHA and RCat-s1 as shown in Fig. 3 when comparing all catalysts under identical conditions at 390 °C. For silicalite, the yield and initial rate of gaseous production was significantly decreased and lower during the course of reaction and the time for plastic waste to be degraded lengthened until the end of total collection time. The maximum rate of generation was observed after 2 min with the zeolite catalysts (ZSM-5 and HUSY), whereas the maximum was observed after 3 min with the zeolite-based RCat-s1 catalyst and SAHA catalysts. The systematic experiments discussed in this work indicate that catalyst deactivation is being produced by active-site coverage, and consequently decrease the activity of the catalyst, giving the reason of decreasing of reaction rate with reaction time.

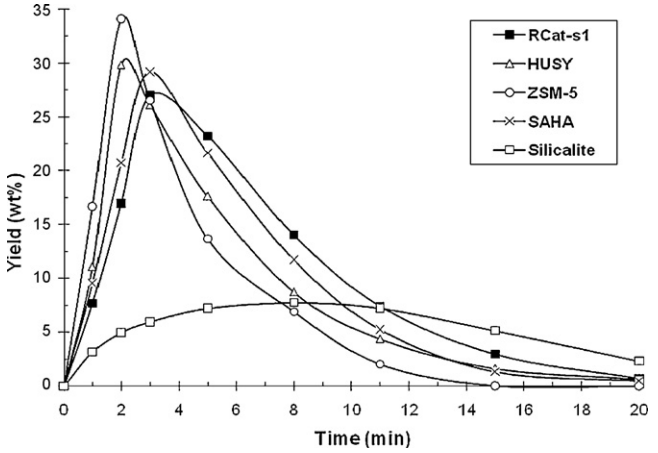

Fig. 3. Comparison of hydrocarbon yields as a function of time for the catalytic degradation of post-consumer waste plastics (WPs#4) at 390 °C over different catalysts (catalyst to plastic ratio = 30 wt%, rate of fluidization gas = 600 ml min^{-1} and catalyst particle size = 125–180 μm).

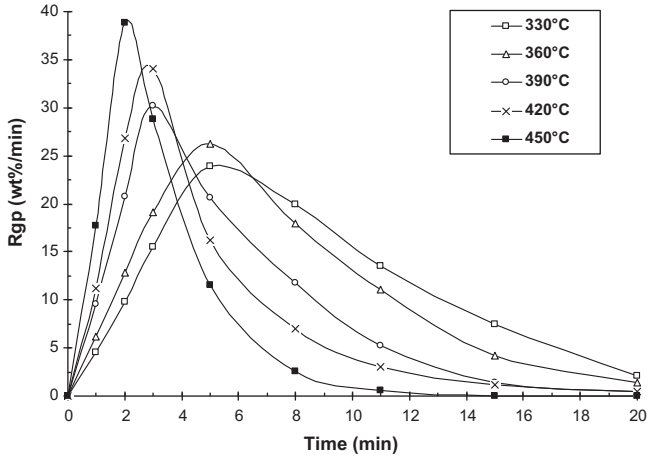

Fig. 4. Comparison of hydrocarbon yields as a function of time at different reaction temperatures for the catalytic degradation of post-consumer waste plastics (WPs#4) over RCat-s1 catalyst (rate of fluidization gas = 600 ml min^{-1}, catalyst to plastic ratio = 30 wt% and catalyst particle size = 125–180 μm).

3.2. Product selectivity variation with reaction conditions

The influence of reaction conditions including reaction temperatures, flow rates of fluidizing gas (300–900 ml min^{-1}) and ratios of plastic waste to catalyst feed has been investigated. The rate of hydrocarbon production as a function of time at five temperatures is compared in Fig. 4 and as expected, faster rates were observed at higher temperatures. At 450 °C, the maximum rate of hydrocarbon production was 37 wt% after only 2 min with all the plastic degraded after approximately 8 min. As the temperature decreased, the initial rate of hydrocarbon production dropped and the time for the polymer to be completely degraded lengthened. At 330 °C, the rate of hydrocarbon production was significantly lower throughout the whole reaction with the polymer being degraded over 20 min. Both acidity and diffusion constraints within individual microp-

Table 2
Summary of the main products of post-consumer waste plastics (WPs#4) degradation at reaction temperature of 390 °C over various cracking catalysts (fluidizing N_2 rate = 600 ml min^{-1}, catalyst to plastic ratio = 30 wt%, catalyst particle size = 125–180 μm and total time of collection = 60 min).

	Catalyst type				
	RCat-s1	Silicalite	HUSY	ZSM-5	SAHA
Yield (wt% feed)					
Gaseous	82.4	13.5	85.6	88.3	84.1
Liquid[a]	3.8	1.4	3.3	3.4	3.6
Residue[b]	11.7	85.1	8.6	6.4	10.5
Involatile residue	9.3	83.2	4.1	4.9	8.4
Coke	2.4	1.9	4.5	1.5	2.1
HCl	2.1	1.4	2.5	1.9	1.8
Distribution of gaseous products (wt% feed)					
Light gases (C_1–C_4)	24.	6.8	35.7	52.7	30.2
Gasoline (C_5–C_9)	54.8	6.2	48.4	34.5	52.4
Styrene	0.7	0.1	0.5	0.6	0.8
BTX[c]	1.6	0.4	1.0	0.5	0.7

[a] Condensate in condenser and captured in filter.
[b] Coke and involatile products.
[c] Benzene, toluene and xylene.

Table 3
Product distributions shown from RCat-s1 catalyzed pyrolysis of waste plastics (WPs#4) at different fluidizing N_2 rates (reaction temperature = 390 °C, fluidizing N_2 rate = 600 ml min^{-1}, catalyst to plastic ratio = 30 wt% and catalyst particle size = 125–180 μm).

	Fluidising N_2 rates (ml min^{-1})				
	900	750	600	450	300
Yield (wt% feed)					
Gaseous	84.6	83.1	82.4	82.1	81.3
Liquid[a]	4.5	4.8	3.8	3.9	3.8
Residue[b]	8.8	9.4	11.7	11.8	12.5
Involatile residue	6.6	7.0	9.3	9.5	10.4
Coke	2.2	2.4	2.4	2.3	2.4
HCl	2.1	2.1	2.1	2.2	2.0
Distribution of gaseous products (wt% feed)					
Light gases (C_1–C_4)	29.7	27.9	24.3	24.1	24.5
Gasoline (C_5–C_9)	53.6	54.0	54.8	55.1	53.6
Styrene	0.5	0.5	0.7	0.8	0.8
BTX[c]	0.8	1.2	1.8	2.1	2.4

[a] Condensate in condenser and captured in filter.
[b] Coke and involatile products.
[c] Benzene, toluene and xylene.

ores of each catalyst may play significant roles in the observed product distribution. The results shown in Fig. 5 illustrate that for efficient plastic waste degradation good mixing is required, with only a slight drop-off in the rate of degradation observed at the lowest fluidizing flow used (300 ml min^{-1}). Furthermore, changing the fluidizing flow rate influences the product distribution. At low flow rates (longer contact times), secondary products are observed with increased amounts of coke precursors (BTX) although the overall degradation rate is slower as shown by increasing amounts of partially involatile residues (Table 3). The amount of RCat-s1 used in the degradation of post-consumer plastic mixture remained constant and, therefore, as more waste plastics was added to the reactor then fewer catalytic sites per unit weight of catalyst were available for cracking. The overall effect of increasing the plastic to catalyst

Table 4
Product distributions shown from RCat-s1 catalyzed pyrolysis of waste plastics (WPs#4) at different ratios of catalyst to plastic waste (reaction temperature = 390 °C, fluidizing N_2 rate = 600 ml min^{-1} and catalyst particle size = 125–180 μm).

	Ratio of catalyst to plastic waste (wt/wt %)				
	60	40	30	20	10
Yield (wt% feed)					
Gaseous	85.5	84.2	82.4	81.5	79.5
Liquid[a]	3.1	3.3	3.8	5.0	5.7
Residue[b]	9.2	10.4	11.7	12.2	13.1
Involatile residue	6.5	7.9	9.3	10.1	11.1
Coke	2.7	2.5	2.4	2.1	2.0
HCl	2.3	2.1	2.1	1.8	1.7
Distribution of gaseous products (wt% feed)					
Light gases (C_1–C_4)	25.5	25.8	24.3	25.4	25.8
Gasoline (C_5–C_9)	58.1	56.3	54.8	52.9	50.8
Styrene	0.8	0.7	0.7	0.5	0.4
BTX[c]	1.1	1.4	1.8	2.2	2.5

[a] Condensate in condenser and captured in filter.
[b] Coke and involatile products.
[c] Benzene, toluene and xylene.

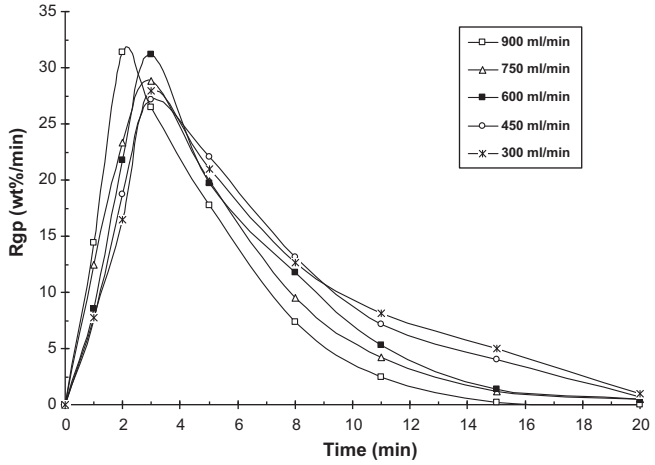

Fig. 5. Comparison of hydrocarbon yields as a function of time at different fluidization gas for the degradation of post-consumer waste plastics (WPs#4) over RCat-s1 catalyst (reaction temperature = 390 °C, catalyst to plastic ratio = 30 wt% and catalyst particle size = 125–180 μm).

ratio from 10:1 to 10:6 on the rate of hydrocarbon generation was small but predictable. As the plastic to catalyst ratio increases, the possibility of post-consumer plastic adhesion to the reactor wall increases as the amount of unconverted plastic waste in the reactor rises. The total product yield after 20 min showed only a slight downward trend even after a 10 fold increase in added plastic waste. This can be attributed to the sufficient cracking ability of RCat-s1 and excellent contact between post-consumer plastic mixture and catalyst particles. Consequently, as more plastic mixture was added, lower C_5–C_9 gasoline and HCl/styrene yields but higher liquid yields and involatile residues were observed (Table 4). In addition, more BTX (coke precursor) was produced but increasing the plastic to catalyst ratio had only virtually no effect on C_1–C_4 hydrocarbon gases productions.

3.3. Kinetic/mechanistic results and discussion

The kinetic model has been used to represent product distributions for the degradation of mixture of post-consumer waste plastics (WPs#4) over acidic cracking catalysts under the fluidized bed reaction. As shown in Fig. 6, it shows that the calculated values using various catalysts are in good agreement with the experimental data. The apparent rate constants based on the model for various catalysts used in this study are summarized in Table 5. The generation of intermediates (long-chain olefins and carbenium ions) from the liquid-phase plastic is much faster than other reaction rates such as the generation of the paraffinic lump (k_{p,c^*}) and the coke/BTX lump ($k_{r/a,c^*}$). The value of k_{i,c^*} is higher for zeolites (ZSM-5 > RCat-s1) than for SAHA. As can be seen in Fig. 6, zeolites gave more intermediate stream about 70 wt% compared with 60 wt% with SAHA. It seems that zeolites of ZSM-5 and RCat-s1 are likely to form a plastic/zeolite complex and consequently to precede the scission reaction further to generate the volatile products. This also suggests that the nature of the catalyst with zeolites is more effective in converting polymers into intermediates of volatile precursors than the amorphous SAHA. The subsequent reactions for the generation the olefinic lump, coke/BTX lump, HCl lump, and paraffinic lump from long-chain olefins and carbenium ions lump was found to vary with the catalyst used. Higher values of the apparent rate constant of paraffinic lump (k_{p,c^*}) and coke/BTX lump ($k_{r/a,c^*}$) were observed in RCat-s1 compared to in ZSM-5 and SAHA. For zeolites of ZSM-5 and RCat-s1, the generation of olefinic and paraffinic lumps is much faster than the generation of coke/BTX lump. For SAHA, the generation of the olefinic

Table 5
Comparison of apparent rate constants and product selectivity for the degradation of post-consumer commingled waste plastics (WPs#4) over different catalysts (reaction temperature = 390 °C, fluidizing N_2 rate = 600 ml min^{-1}, catalyst to plastic ratio = 30 wt% and catalyst particle size = 125–180 μm).

Catalyst	k_{i,c^*} ($\times 10^{-2}$ min^{-1})	$K_{c/a,c^*}$ ($\times 10^{-2}$ min^{-1})	k_{p,c^*} ($\times 10^{-3}$ min^{-1})	k_{h,c^*} ($\times 10^{-3}$ min^{-1})	$k_{o,i}$ ($\times 10^{-2}$ min^{-1})	$k_{p,i}$ ($\times 10^{-2}$ min^{-1})	$k_{c/a,i}$ ($\times 10^{-2}$ min^{-1})	$k_{h,i}$ ($\times 10^{-3}$ min^{-1})	$k_{o,i}/k_T{}^a$ (%)	$k_{p,i}/k_T$ (%)	$k_{c/a,i}/k_T$ (%)	$k_{h,i}/k_T$ (%)
RCat-s1	210.7	9.4	4.3	1.1	17.9	13.8	2.5	0.8	51.1	39.5	7.2	2.3
ZSM-5	245.5	3.9	1.7	1.2	24.1	9.6	0.8	0.7	68.5	25.9	2.3	1.9
SAHA	180.4	15.7	2.8	0.7	21.9	5.2	2.3	0.5	77.3	17.4	7.7	1.7

$k_T{}^a = k_{o,i} + k_{c/a,i} + k_{p,i} + k_{h,i}$

Table 6
Comparison of product selectivity for the degradation of post-consumer commingled waste plastics (WPs#4) over different particle size of RCat-s1 catalysts in the temperature range 330–450 °C using the lumping model (fluidizing N_2 rate = 600 ml min^{-1} and catalyst to polymer ratio = 30 wt%).

Temperature (°C)	RCat-s1-L (125–180 μm)				RCat-s1-S (75–120 μm)			
	$k_{o,i}/k_T^a$ (%)	$k_{c/a,i}/k_T$ (%)	$k_{p,i}/k_T$ (%)	$k_{h,i}/k_T$ (%)	$k_{o,i}/k_T^a$ (%)	$k_{c/a,i}/k_T$ (%)	$k_{p,i}/k_T$ (%)	$k_{h,i}/k_T$ (%)
330	43.7	5.4	49.5	1.4	46.2	4.3	48.0	1.5
360	41.5	4.9	52.0	1.6	43.8	4.0	50.7	1.5
390	39.7	4.3	54.1	1.9	41.3	3.6	53.4	1.7
430	36.6	3.9	57.4	2.1	39.1	3.3	55.7	1.9
450	41.9	3.6	52.2	2.3	43.2	3.1	51.6	2.1

$k_T^a = k_{o,i} + k_{c/a,i} + k_{p,i} + k_{h,i}$.

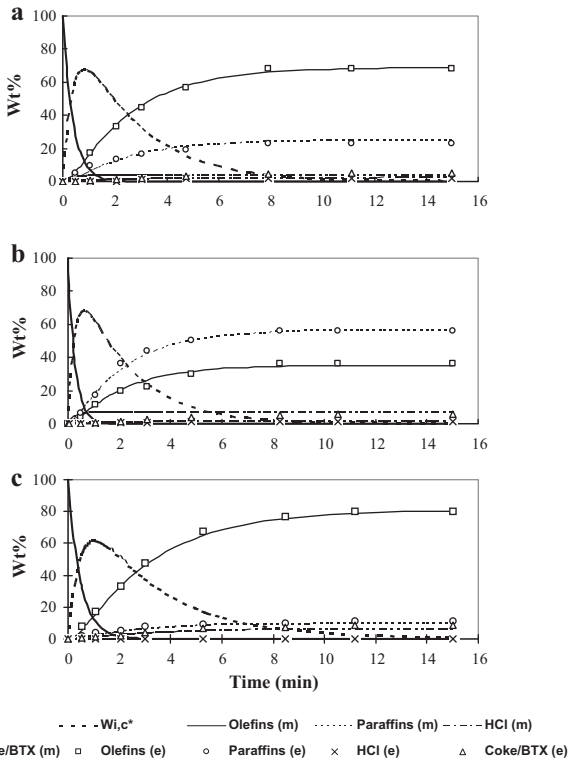

Fig. 6. Comparison of calculated (m) and experimental (e) results for the degradation of postconsumer waste plastics (WPs#4) over (a) ZSM-5, (b) RCat-s1 and (c) SAHA catalysts at 390 °C (catalyst particle size = 125–180 μm, fluidizing N2 rate = 600 ml min^{-1} and catalyst to plastic ratio = 30%, wt/wt).

lump ($k_{o,i}$) is much faster than the other values of the generation of paraffinic lump ($k_{p,i}$) and HCl lump ($k_{h,i}$). The difference in the amount of olefinic products ($k_{o,i}/k_T$) for different catalysts is in the order SAHA (77.3%) > ZSM-5 (68.5%) ≫ RCat-s1 (51.1%). However, the higher value of paraffinic lump ($k_{p,i}$) for RCat-s1 (39.5%) was obtained compared to the cases of ZSM-5 and SAHA. The difference in product selectivity for zeolites can be seen with RCat-s1 giving a higher selectivity for paraffins than ZSM-5. However, ZSM-5 generates a much higher selectivity for olefins compared with RCat-s1. These results may reflect RCat-s1 containing potentially cracking activity with bimodal pore structures, which is composed of both the micropore of zeolite and the mesopore of silica-alumina used in the FCC catalyst matrix, and can provide the unzipping ability when they are enough accessible to the reactant and may allow bulky reactions to occur, ultimately leading to the generation of paraffinic products with substantial coke/BTX levels (7.1%). Amorphous SAHA with large mesopores and low acidity resulted in a relatively low rate of bimolecular reaction to further react to produce paraffins (17.4%) with lower level of HCl content (1.7%). In contrast, ZSM-5 with narrower pore openings (0.55 nm × 0.51 nm) and no supercages, the bulky feed molecules have restricted access to the internal active catalytic sites and special restrictions within the pore system tend to inhibit the bimolecular processes leading to lower values of coke/BTX production (2.3%) in this study. Both acidity and diffusion constraints within individual micropores of each catalyst may play significant roles in the observed product distribution. As can be seen in Table 1, the acidity order found in this work is the following: ZSM-5 > SAHA > RCat-s1 > silicalite. As expected, the sodium forms of siliceous ZSM-5, silicalite, containing very few or no catalytically active sites (Si/Al > 1000), give very low conversions of plastic wastes to volatile hydrocarbons compared with other acid solids. On the other hand, the weaker acid properties exhibited by SAHA, compared to zeolitic materials, were compensated in part

by their larger pore size. Despite the strong acid properties, ZSM-5 showed the similar catalytic activity of all acid solid for the degradation of post-consumer PE/PP/PVC/PS waste plastics. This behavior was attributed to steric impediments related to its microporous textile that hinder the access of large polymer molecules to its internal acid sites. However, the modified FCC spent catalyst (RCat-s1) was to provide an alternative option in all cracking catalysts as it combined a strong acid character with favorable accessibility into its active sites due to its bimodal microstructures. Therefore, the important factor determining the catalytic acidity of these materials is the acidity, and the results obtained in this work present that the activity of the solid acid catalyst increases as the acidity increases. Furthermore, the catalytic role of the acid sites will only be observed if the reactant molecules access to the active sites located in the interior of the pores.

The rate constants for the catalytic degradation of post-consumer waste plastics (WPs#4) over RCat-s1 with particle sizes of 125–180 μm and 75–120 μm at five different temperatures (330–450 °C) are listed in Table 6. The selectivity toward the olefinic products ($k_{o,i}/k_T$) as a function of reaction temperature shows that the amount of olefins decreased with increasing reaction temperature from 330 to 430 °C then increased at 450 °C. On the other hand, the results show the paraffinic products ($k_{p,i}/k_T$) occurred at 430 °C rather than at the higher temperature of 450 °C. It could be the case that selectivity products of paraffinic fraction increased with increasing reaction temperature and olefinic fraction decreased with an increase in temperature below 430 °C. But at higher temperature (450 °C), the degradation of commingled plastic waste to volatile products may precede both by catalytic and thermal reactions leading to the variation of product distributions. An interesting parameter derived from these results is the threshold temperature around 430 °C in Table 6 at which start to express significant catalytic activity for the cracking of the plastic mixture. The selectivity toward the olefinic products ($k_{o,i}/k_T$) as a function of reaction temperature shows that the amount of olefins decreased with increasing reaction temperature from 330 to 430 °C then increased at 450 °C. On the other hand, the results show the paraffinic products ($k_{p,i}/k_T$) occurred at 430 °C rather than at the higher temperature of 450 °C. Moreover, these results also exhibit a trend toward HCl ($k_{h,i}/k_T$) products at increasing reaction temperature. On the contrary, the proportion of undergoes a slight decline with the temperature, whereas its content in coke/BTX ($k_{c/a,i}/k_T$) grows to about 3% at 450 °C. The external surface of the catalysts is an important factor controlling activity and selectivity. From values of $k_{o,i}/k_T$ and $k_{c/a,i}/k_T$, the smaller particle RCat-s1-S catalyst (75–120 μm) shows a higher selectivity for olefins (39.1–46.2% vs. 36.6–43.7%) and a lower selectivity for coke/BTX (3.1–4.3% vs. 3.6–5.4%) than the larger particle RCat-s1-L catalyst (125–180 μm). The result appears that the feed can be cracked at or close to the external surface of the catalyst and therefore, the controlling catalytic parameters will be not only the total number of acid sites but also the number of accessible ones related to the particle size selected.

4. Conclusion

A catalytic fluidizing reaction system has been used to obtain a range of volatile hydrocarbons by catalytic degradation of mixture of post-consumer waste plastics (WPs#4) in the temperature range 330–450 °C. In this work, a similar FCC process with the fluidized-bed reactor system has been shown to have a number of advantages in the catalytic pyrolysis of commingled plastic waste; it is characterized by excellent heat and mass transfer, much less prone to clogging with molten polymer and gives a nearly constant temperature throughout the reactor. The catalytic degradation of plastic waste over the recycled/modified commercial FCC spent catalyst (RCat-s1) using fluidizing cracking reactions was shown to be a useful method for the production of potentially valuable hydrocarbons. A combined kinetic and mechanistic model giving chemical information, applicable to the fluidized-bed reactions, was used to predict production rates and product selectivity for the catalytic degradation of commingled plastic waste. The model gives a good representation of product selectivity and product distributions for catalytic plastic recycling and also provides an improvement of the empirical "lumping" techniques. This paper outlines some recent results relevant to the conversion of post-consumer waste plastics for the production of potentially valuable hydrocarbons and also attempts to apply a model for the mechanism and kinetics of catalytic degradation of waste plastics. It is also concluded that the results of this study are useful for determining the effects of catalyst types and reaction conditions on both the product distribution and selectivity from commingled plastic waste, and especially for the utilization of a post-use catalyst for producing valuable hydrocarbons in a fluidizing cracking process.

Acknowledgements

The authors would like to thank the National Science Council (NSC) of the Republic of China (R.O.C.) and Kingdom Resource Technologic Co. Ltd. for those kindly financial supports (NSC 99-2221-E-244-010 and 99G-59-013).

References

[1] N.C. Billingham, Polymers and the Environment Gerald Scott, Royal Society of Chemistry, London, 1999.
[2] J. Brandrup, M. Bittner, W. Michaeli, G. Menges, Recycling and Recovery of Plastics, Carl Hanser Verlag, Munich/New York, 1996.
[3] P.N. Sharratt, Y.H. Lin, A. Garforth, J. Dwyer, Ind. Eng. Chem. Res. 36 (1997) 5118.
[4] Y. Uemichi, J. Nakamura, T. Itoh, A. Garforth, J. Dwyer, Ind. Eng. Chem. Res. 38 (1999) 385.
[5] Y.H. Lin, M.H. Yang, Appl. Catal. A: Gen. 328 (2007) 132.
[6] S.C. Cardona, A. Corma, Appl. Catal. B: Environ. 25 (2000) 151.
[7] A. Dawood, Miura, Polym. Degrad. Stab. 76 (2002) 45.
[8] K. Gobin, G. Monos, Polym. Degrad. Stab. 86 (2004) 225.
[9] B. Saha, A.K. Ghoshal, Ind. Eng. Chem. Res. 46 (2007) 5485.
[10] Y.H. Lin, M.H. Yang, J. Mol. Catal. A: Chem. 231 (2005) 113.
[11] A. Marcilla, A. Gomez Siurana, F. Valdes, J. Anal. Appl. Pyrol. 79 (2007) 433.
[12] G. de la Puente, U. Sedran, C. Klocker, Appl. Catal. B: Environ. 36 (2002) 279G; Puente, C. Klocker, U. Sedran, Appl. Catal. B: Environ. 36 (2002) 279.
[13] Z. Gao, K. Ksuyoshi, I. Amasaki, M. Nakada, Polym. Degrad. Stab. 80 (2003) 269.
[14] S. Ali, A.A. Garforth, D.H. Harris, D.J. Rawlence, Y. Uemichi, Catal. Today 75 (2002) 247.
[15] K.H. Lee, D.H. Shin, Y.H. Seo, Polym. Degrad. Stab. 84 (2004) 123.
[16] Y.H. Lin, M.H. Yang, J. Anal. Appl. Pyrol. 83 (2008) 101.
[17] J. Aguado, D.P. Serrano, J.M. Escola, Ind. Eng. Chem. Res. 47 (2008) 7892.
[18] X. Feng, W.K. Hall, J. Catal. 166 (1997) 368.
[19] Y.H. Lin, M.H. Yang, Thermochim. Acta 471 (2008) 52.